

OBSERVATIONS OF TITAN'S MESOSPHERE

C. A. GRIFFITH AND P. PENTEADO

Department of Planetary Sciences, University of Arizona, 1629 East University Boulevard, Tucson, AZ 85721; griffith@lpl.arizona.edu,
penteado@lpl.arizona.edu

T. K. GREATHOUSE¹

Lunar and Planetary Institute, 3600 Bay Area Boulevard, Houston, TX 77058-1113; greathouse@lpi.usra.edu

H. G. ROE¹

Division of Geological and Planetary Sciences, Mail Code 170-25, California Institute of Technology,
1200 East California Boulevard, Pasadena, CA 91125; hroe@gps.caltech.edu

AND

R. V. YELLE

Department of Planetary Sciences, University of Arizona, 1629 East University Boulevard,
Tucson, AZ 85721; yelle@lpl.arizona.edu

Received 2004 December 8; accepted 2005 July 6; published 2005 July 28

ABSTRACT

We have recorded spectra of Titan's ν_4 band of CH_4 at a higher resolving power ($R = 70,000$) than prior measurements to better constrain the thermal structure of Titan's atmosphere from 100 to 600 km altitude. Radiative transfer analyses of the spectra indicate a temperature profile below 300 km that is consistent with past measurements. The high resolving power of our observations provides the first infrared measurement of Titan's thermal structure between 300 and 600 km. We detect the presence of a mesosphere, with a drop of temperature above 380^{+50}_{-100} km altitude of at least 15 K, consistent with radiative cooling of the atmosphere by emission from hydrocarbons.

Subject headings: infrared: solar system — planets and satellites: general — radiative transfer — techniques: spectroscopic

1. INTRODUCTION

Titan's thermal profile reveals the partitioning of solar energy within the atmosphere and manifests the radiative, convective, and conductive processes by which the atmosphere cools. Titan's temperatures have been measured below 250 km altitude by *Voyager* radio occultation measurements coupled with the analysis of CH_4 ν_4 emission lines (Lindal et al. 1983; Lellouch et al. 1989; Coustenis et al. 1989, 2003; Lellouch et al. 1990). These observations are readily explained by radiative equilibrium models of Titan's atmosphere (Samuelson 1983; McKay et al. 1989); Titan's troposphere cools mainly radiatively, giving rise to a decreasing temperature profile up to the tropopause at 40 km altitude. Between 50 and 200 km, the atmosphere warms as a result of the absorption of sunlight by haze and methane. At 200 km, radiative cooling to space competes with radiative warming, giving rise to a nearly isothermal temperature profile of ~ 176 K up to roughly 350 km altitude (McKay et al. 1989; Yelle 1991). Occultation measurements, which probe levels between 250 and 500 km, reveal an average temperature cooler than 170 K and warmer than 150 K (Hubbard et al. 1993) and further disclose temperature oscillations with altitude, suggestive of gravity waves (Sicardy et al. 1999). Radiative-conductive models indicate that Titan's atmosphere cools above 350 km from emission by C_2H_6 and other hydrocarbons to form a mesopause at ~ 550 km (Yelle 1991). The nature of Titan's thermal profile, whether isothermal from 300 to 600 km or possessing a mesosphere, was not ascertained by past observations.

Here we present spectra of Titan's ν_4 band at higher resolution ($R \sim 70,000$, or 0.018 cm^{-1} at 1230 cm^{-1}) than prior

measurements. These spectra do not completely resolve the lines, whose Doppler widths are 0.0014 cm^{-1} , for example, at 181 K. Nonetheless, the data separate most emission lines, thereby providing a measure of their individual intensities (Fig. 1). The high resolution allows us to probe the atmospheric structure over the broad altitude range of 100–600 km. Using lines of a variety of intensities, we study independently the thermal profile below 200 km (probed by the weakest lines and line wings), that between 200 and 400 km (probed by intermediate lines), and that between 400 and 600 km (sampled by the strongest lines). Most interesting is the capability of our data to probe Titan's thermal profile above 300 km, which is not possible with prior, lower resolution observations.

2. OBSERVATIONS

We recorded disk-integrated spectra of Titan on 2004 October 7, 11, and 12 using NASA's Infrared Telescope Facility, equipped with the Texas Echelon Cross-dispersed Echelle Spectrograph (TEXES; Lacy et al. 2002). The spectra cover the $1228\text{--}1239 \text{ cm}^{-1}$ wavenumber interval and have a resolving power of $R \sim 70,000$. The data were flux-calibrated with α CMi (on October 7) and α CMa (on October 7, 11, and 12), stars at similar air mass to Titan, with an accuracy estimated to be 10%–20%. The telluric transmission, determined with the spectrum of α CMa (Fig. 1), confirms that Titan's methane lines were Doppler shifted by -30 km s^{-1} from terrestrial methane lines. The data were reduced following the techniques described by Lacy et al. (2002).

3. ANALYSIS

We analyze the observations with radiative transfer calculations that produce synthetic spectra based on an assumed

¹ Visiting Astronomer, NASA Infrared Telescope Facility, Mauna Kea, Hawaii.

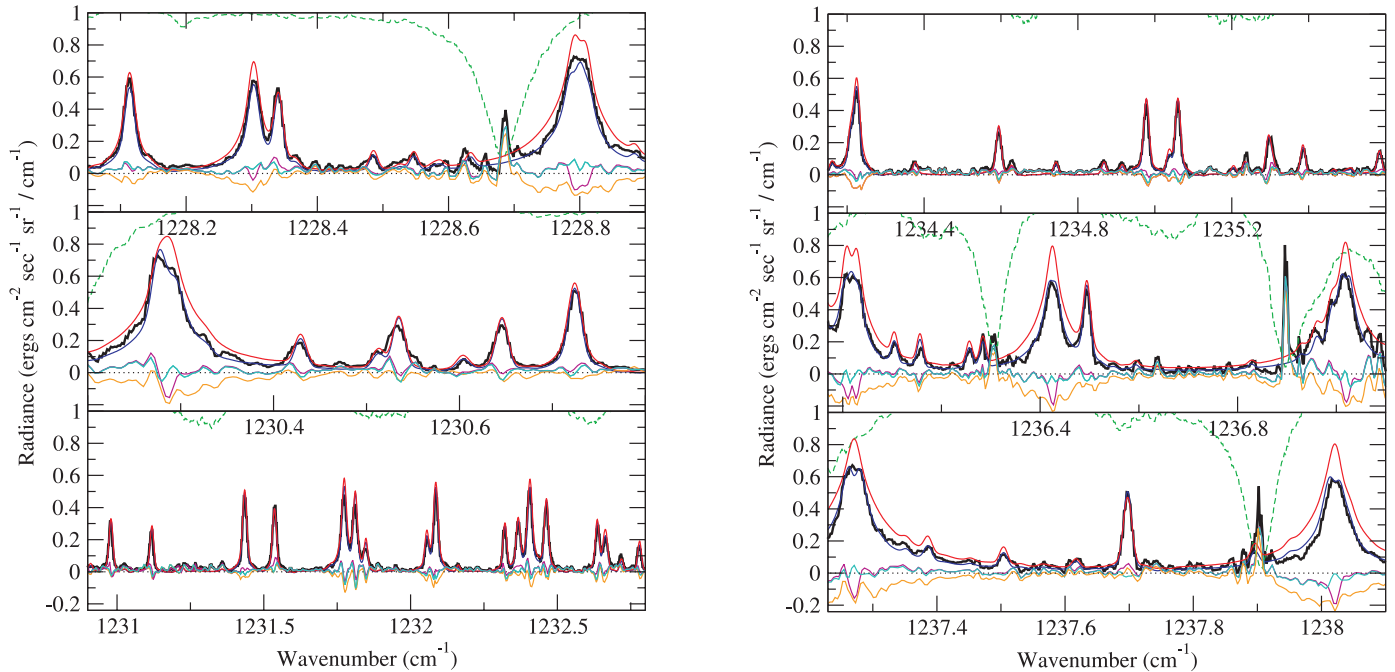


FIG. 1.—Observations (black) shown with synthetic spectra, calculated with 1.9% CH₄ and our nominal thermal profile (blue) and the initial profile (red), depicted in Fig. 2. The differences between the models and observations are shown in cyan and orange, respectively. The magenta line indicates the residuals between the observations and a model (not shown) produced from a thermal profile similar to the best-fit model below 300 km and, above 300 km, an isotropic profile of 176 K. Terrestrial atmospheric transmission appears as the dashed green line. The 1230.8–1231 and 1232.7–1234.2 cm⁻¹ regions are not included because they contain only very few features. The 1235.6–1236.2, 1228.9–1230.2, and 1237–1237.2 cm⁻¹ spectral regions are heavily corrupted by terrestrial lines and thus omitted.

atmospheric temperature profile. Non-LTE calculations for Titan's conditions indicate that local thermodynamic equilibrium, the assumption for our present calculations, provides a good approximation. A collision de-excitation probability of 1.4×10^{-6} for the ν_4 band implies that the radiative and collisional de-excitation rates are equal at $\sim 1 \mu\text{bar}$; however, non-LTE calculations show that the source function is still within 10% of the Planck function at 0.1 μbar because of the combined

effects of radiation trapping and pumping by solar photons absorbed in higher energy bands. Intensity calculations for emission and solar incident angles of 60° show that the LTE and non-LTE results agree to within 2.4% for the spectral range considered here.

Absorption coefficients of CH₄ and CH₃D are determined from the line parameters of methane from the HITRAN database (Rothman et al. 2003), using line-by-line techniques and assuming a Voigt line profile. We modeled the few CH₃D lines with a CH₃D/CH₄ ratio of 55×10^{-5} , following the results of Penteado et al. (2005). The ¹³CH₄ lines were analyzed assuming the terrestrial isotopic ratio (1.116×10^{-2}).

We initially assume a simple profile that is consistent with *Voyager* radio occultation measurements below 200 km altitude (Lellouch et al. 1989), above which temperatures rise to 176 K at ~ 300 km altitude, following the thermal profile calculated by Yelle et al. (1997). Between 300 and 700 km we adopted a constant temperature of 176 K (Fig. 2), which provides a standard temperature for evaluating the intensities of the emission lines formed in Titan's high stratosphere. This initial model overestimates the emissions from strong lines that probe highest in the stratosphere (between 400 and 600 km), in addition to the line wings, which probe the lower stratosphere (100–200 km altitude). This behavior can be seen, for example, in the 1237.2 cm⁻¹ methane line, from the spectral models (Fig. 1) and the corresponding contribution functions (Fig. 3). Emission from intermediate-strength lines, which sample altitudes of 200–400 km, are fitted fairly well and occasionally underestimated by our initial model, as shown by the emission feature at 1237.7 cm⁻¹ (Fig. 1, right). In addition, the strongest lines have flattened peaks, indicative of a central absorption and thus the presence of a mesosphere (Fig. 1), which are not reproduced by our model.

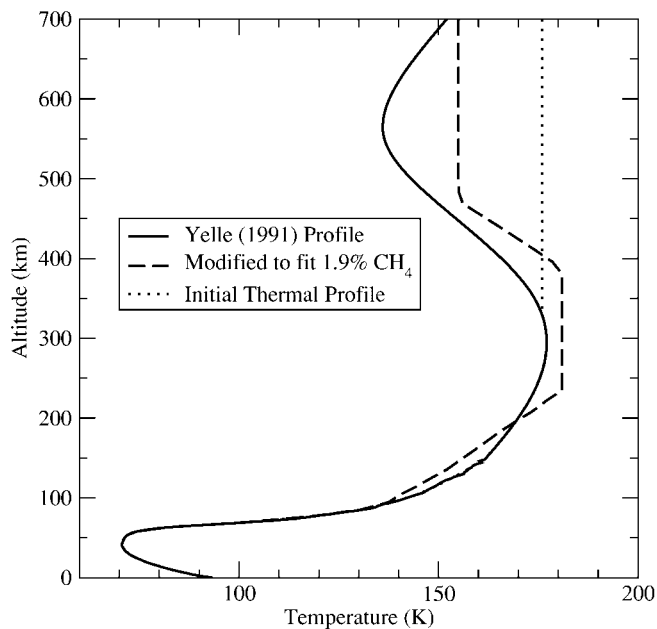


FIG. 2.—Our initial profile (dotted line) and our nominal, or best-fit, thermal profile (dashed line) compared with the profile of Yelle (1991).

We therefore modified the initial thermal profile by decreasing the temperature above an altitude that we designate the bottom of the mesosphere (Z_M) and increasing the temperature from this altitude down to that which we designate the stratosphere altitude (Z_S). We assume a constant temperature between Z_S and Z_M , which we call the stratosphere temperature, and a constant temperature above Z_M , which we call the mesosphere temperature. This simplified model was adopted because we do not have information on the detailed structure of the profile within these regions.

We can fit the data well if $Z_M = 380^{+50}_{-100}$ km and $Z_S = 230 \pm 20$ km. Spectra calculated with the nominal resultant thermal profile that best matches the data are shown in Figure 1 (*blue*), along with the residuals between the calculated and observed spectra (*cyan*). Also depicted are the residuals (*magenta*) between the observations and a model (not shown) calculated with an adjusted temperature in the lower atmosphere (below 300 km) and no mesosphere (Fig. 1). Contribution functions (Fig. 3) indicate that the temperature above ~ 380 km must be low enough so that little to no emission above this level contributes to the formation of Titan's strongest ν_4 lines; this requirement sets the upper limit for Z_M . The lower limit is set by the need to match the strong and intermediate lines simultaneously, as well as the widths of the intermediate lines. The value of Z_S controls the wings of the strong lines, as well as the relative strengths of the strong and intermediate lines. If this "isothermal" region is expanded (or contracted), its temperature must be diminished (or increased) to fit the lines. A limited range of values work.

To determine the highest mesosphere temperature that is consistent with the data, we ran a series of models in which we decreased the stratospheric temperature while increasing the mesospheric temperature. A mesospheric temperature as high as 162 K and a stratospheric temperature as low as 177 K provide the limiting temperatures that agree with the data. Higher mesospheric temperatures, together with lower stratospheric temperatures (needed to fit the strong lines), fail to match both strong and intermediate lines to within 10%. Thus, Titan has a mesosphere that is at least 15 K cooler than the stratosphere below. A lower limit to Titan's mesosphere is difficult to establish. The strong-line energy states become depopulated as the temperature goes from 155 K to 100 K. This decrease in optical depth causes the center of line emission to move down to lower altitudes (~ 400 km) near the boundary between the mesosphere and stratosphere. The uncertainty in the profile compromises our ability to constrain the lowest mesosphere temperature. Nonetheless, we find that the models that best interpret the data have unity optical depth at altitudes with temperatures exceeding 145 K.

The stratospheric methane abundance is only loosely constrained. Analysis of the *Voyager* radio occultation measurements coupled with *Voyager* Infrared Interferometer Spectrometer (IRIS) observations ($R \sim 270$) of ν_4 methane emissions suggest mixing ratios of 1%–1.7% for an argon-free atmosphere (Lellouch et al. 1989). Reanalyses of IRIS data indicate 1%–3.5% CH_4 (Courtin et al. 1995; Samuelson et al. 1997). We investigated the effects of the methane abundance on the derived temperature profile by considering methane mixing ratios of 1% and 3% and varying the temperature profile (derived assuming 1.9% methane) in the stratosphere and mesosphere to match the data. A decrease (or increase) in the methane abun-

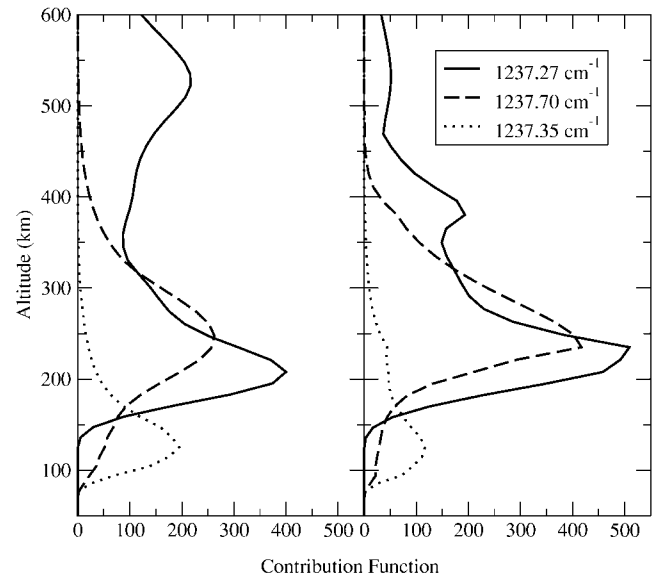


FIG. 3.—Contribution functions of a strong line (1237.27 cm^{-1}), line wing (1237.35 cm^{-1}), and intermediate-strength line (1237.70 cm^{-1}), integrated over the point-spread function, for our initial temperature profile (*left*) and nominal temperature profile (*right*).

dance to 1% (or 3%) causes a decrease (or increase) in the flux of the wings and peaks of strong lines. Variations in the methane abundance affect predominantly the emission at altitudes where both the thermal profile is steepest and the contribution function largest; that is at 100–230 km. An increase in the temperature by 3 K at 100–230 km above our nominal profile fits the data well for a 1% CH_4 atmosphere, while a 3 K decrease in the temperature at these levels matches the observations for 3% CH_4 . Both 1% and 3% methane abundances indicate a mesosphere temperature 15 K lower than that in the stratosphere.

4. DISCUSSION

Titan's emission spectrum at high resolving power reveals the gross characteristics of Titan's thermal profile at altitudes ranging from 100 to 600 km. The "disk-averaged" temperatures derived for altitudes between 100 and 230 km agree with those determined from lower resolution data (Coustenis et al. 2003) and are cooler than the equatorial profile established by *Voyager* radio data (Lellouch et al. 1989). Our cooler temperatures are consistent with the 12 K drop in temperature from the equator to 60° latitude observed by *Voyager* (Flasar & Conrath 1990; Coustenis & Bézard 1995). Our observations further indicate a "disk-averaged" temperature of 180 ± 2 K for Titan's stratosphere at ~ 250 – 350 km, a little warmer than the nominal model of Yelle et al. (1997), while consistent with the analysis of Coustenis et al. (2003). Moreover, Titan's spectrum reveals evidence for a mesosphere above 380^{+50}_{-100} km altitude at least 15 K cooler than the atmosphere below. This altitude and cooler temperature can be explained by radiative cooling by C_2H_6 and other hydrocarbons (Yelle 1991).

This research is supported by the NASA Planetary Astronomy Program, grant NAG 5-12272. The TEXES observations were funded by NSF grant AST 02-05518 and NASA's Infrared Telescope Facility. We thank the anonymous reviewer for helpful comments.

REFERENCES

- Courtin, R., Gautier, D., & McKay, C. P. 1995, *Icarus*, 114, 144
- Coustenis, A., & Bézard, B. 1995, *Icarus*, 115, 126
- Coustenis, A., Bézard, B., & Gautier, D. 1989, *Icarus*, 80, 54
- Coustenis, A., Salama, A., Schulz, B., Ott, S., Lellouch, E., Encrenaz, T., Gautier, D., & Feuchtgruber, H. 2003, *Icarus*, 161, 383
- Flasar, F. M., & Conrath, B. J. 1990, *Icarus*, 85, 346
- Hubbard, W. B., et al. 1993, *A&A*, 269, 541
- Lacy, J. H., Richter, M. J., Greathouse, T. K., Jaffe, D. T., & Zhu, Q. 2002, *PASP*, 114, 153
- Lellouch, E., Coustenis, A., Gautier, D., Raulin, F., Dubouloz, N., & Frère, C. 1989, *Icarus*, 79, 328
- Lellouch, E., Hunten, D. M., Kockarts, G., & Coustenis, A. 1990, *Icarus*, 83, 308
- Lindal, G. F., Wood, G. E., Hotz, H. B., Sweetnam, D. N., Eshleman, V. R., & Tyler, G. L. 1983, *Icarus*, 53, 348
- McKay, C. P., Pollack, J. B., & Courtin, R. 1989, *Icarus*, 80, 23
- Penteado, P., Griffith, C. A., Greathouse, T. K., & de Bergh, C. 2005, *ApJL*, submitted
- Rothman, L. S., et al. 2003, *J. Quant. Spectrosc. Radiat. Transfer*, 82, 5
- Samuelson, R. E. 1983, *Icarus*, 53, 364
- Samuelson, R. E., Nath, N. R., & Borysow, A. 1997, *Planet. Space. Sci.*, 45, 959
- Sicardy, B., et al. 1999, *Icarus*, 142, 357
- Yelle, R. V. 1991, *ApJ*, 383, 380
- Yelle, R. V., Strobell, D. F., Lellouch, E., & Gautier, D. 1997, in *Huygens Science Payload and Mission* (ESA SP-1177) (Noordwijk: ESA), 243